First published August 31, 2011; doi:10.1152/ajprenal.00665.2010.

COX-2 disruption leads to increased central vasopressin stores and impaired urine concentrating ability in mice

Rikke Nørregaard,[1,2]* Kirsten Madsen,[3]* Pernille B. L. Hansen,[3] Peter Bie,[3] Sugarna Thavalingam,[3] Jørgen Frøkiær,[1,2] and Boye L. Jensen[3]

[1]*The Water and Salt Research Center and* [2]*Institute of Clinical Medicine, University of Aarhus, Aarhus; and* [3]*Cardiovascular and Renal Research, University of Southern Denmark, Odense, Denmark*

Submitted 12 November 2010; accepted in final form 25 August 2011

Nørregaard R, Madsen K, Hansen PB, Bie P, Thavalingam S, Frøkiær J, Jensen BL. COX-2 disruption leads to increased central vasopressin stores and impaired urine concentrating ability in mice. *Am J Physiol Renal Physiol* 301: F1303–F1313, 2011. First published August 31, 2011; doi:10.1152/ajprenal.00665.2010.—It was hypothesized that cyclooxygenase-2 (COX-2) activity promotes urine concentrating ability through stimulation of vasopressin (AVP) release after water deprivation (WD). COX-2-deficient (COX-$2^{-/-}$, C57BL/6) and wild-type (WT) mice were water deprived for 24 h, and water balance, central AVP mRNA and peptide level, AVP plasma concentration, and AVP-regulated renal transport protein abundances were measured. In male COX-$2^{-/-}$, basal urine output and water intake were elevated while urine osmolality was decreased compared with WT. Water deprivation resulted in lower urine osmolality, higher plasma osmolality in COX-$2^{-/-}$ mice irrespective of gender. Hypothalamic AVP mRNA level increased and was unchanged between COX-$2^{-/-}$ and WT after WD. AVP peptide content was higher in COX-$2^{-/-}$ compared with WT. At baseline, plasma AVP concentration was elevated in conscious chronically catheterized COX-$2^{-/-}$ mice, but after WD plasma AVP was unchanged between COX-$2^{-/-}$ and WT mice (43 ± 11 vs. 70 ± 16 pg/ml). Renal V2 receptor abundance was downregulated in COX-$2^{-/-}$ mice. Medullary interstitial osmolality increased and did not differ between COX-$2^{-/-}$ and WT after WD. Aquaporin-2 (AQP2; cortex-outer medulla), AQP3 (all regions), and UT-A1 (inner medulla) protein abundances were elevated in COX-$2^{-/-}$ at baseline and further increased after WD. COX-$2^{-/-}$ mice had elevated plasma urea and creatinine and accumulation of small subcapsular glomeruli. In conclusion, hypothalamic COX-2 activity is not necessary for enhanced AVP expression and secretion in response to water deprivation. Renal medullary COX-2 activity negatively regulates AQP2 and -3. The urine concentrating defect in COX-$2^{-/-}$ is likely caused by developmental glomerular injury and not dysregulation of AVP or collecting duct aquaporins.

aquaporins; PGE_2; water deprivation

MICE DEFICIENT IN PGE_2 EP1 receptor signaling display a mild urine concentrating defect that is coupled to a lower vasopressin (AVP) mRNA level in the hypothalamus (30). However, the source of PGE_2 that potentially activates the EP1 receptor in the neurons of hypothalamic nuclei to promote AVP expression and secretion is not clear. Cyclooxygenase type 2 (COX-2) which is expressed in the hypothalamus (10), is a rapidly inducible enzyme isoform that is a likely candidate. Intracerebroventricular application of the nonselective COX inhibitor meclofenamate impairs hyperosmolality-induced AVP secretion (49). Hypothalamic supraoptic nucleus (SON) neurons are sensitive to experimental addition of prostanoids, particularly PGE_2 and $PGF_{2\alpha}$ (46), which promotes electric and secretory activity. It is not known whether hypothalamic COX-2 activity is regulated by physiological variations in plasma osmolality and supports AVP secretion. There is a paucity of data on the role of COX-2 in the integrated control of urinary concentration. Dietary NaCl loading, dDAVP infusion, and water deprivation (WD) stimulate COX-2 expression in renal medullary interstitial cells (29), which leads to formation of primarily PGE_2 (41) and promotes interstitial cell survival (22). Basolateral exposure of isolated collecting ducts to PGE_2 antagonizes AVP-mediated stimulation of water uptake while it stimulates water flux in the absence of AVP (25). COX-2-generated prostanoids promote medullary blood flow (8) and suppresses Na-K-2Cl cotransporter (NKCC2) expression (21), which would diminish urine concentration by effects on medullary osmolality. At the systemic level, data are also conflicting; deletion of phopholipase A_2 (12) and prostanoid receptors (EP1, EP3) (18, 30) either had no demonstrable effect or, paradoxically, decreased urine concentration (12), indicating that the COX pathway normally supports urine concentration. Nonselective inhibition of COX by indomethacin increased sodium retention and urine concentration in one study (1) but had the opposite effect in another study (4). Gene deletion of COX-2 provides an alternative way to address the issue. However, global COX-2 deletion results in developmental kidney injury with fewer cortical nephrons, while basal diuresis and urine osmolality are not altered (40). Because no central nervous system abnormalities have been described in mice with disrupted COX-2 (COX-$2^{-/-}$), we considered the model well suited to an investigation of regulation of the vasopressin axis by physiological challenges. The primary aim of the present study was to elucidate the role of COX-2 in the control of AVP expression, peptide storage, and release as well as its effect on urine concentrating ability. Using WD as a stimulus, mice with targeted deletion of COX-2 and their wild-type (WT) littermates were studied to determine water and NaCl balance, associated AVP concentrations in plasma and hypothalamic tissue, and AVP-regulated target protein in kidney tissue. These proteins included the V2 receptor (V2R), NKCC2 protein, and collecting duct aquaporins (AQP2 and 3). Because the severity of renal developmental injury is strain specific (51), mice bred on a pure C57BL/6 background, which have a comparably mild phenotype, were chosen for the study. Gender differences in renal phenotype have previously been reported in COX-2-disrupted mice (51), and therefore both male and female mice were included.

* R. Nørregaard and K. Madsen contributed equally to this study.

Address for reprint requests and other correspondence: R. Nørregaard, The Water and Salt Research Center, Institute of Clinical Medicine, Univ. of Aarhus, Aarhus Univ. Hospital-Skejby, Brendstrupgaardsvej 100, DK-8200 Aarhus N, Denmark (e-mail: rikke.norregaard@ki.au.dk).

METHODS

COX-2 knockout mice. COX-2$^{-/-}$ mice on a mixed 129/C57BL/6 background were originally generated by Dinchuk et al. (11). The breeder pairs were obtained from Jackson Laboratories (Bar Harbor, ME) on a predominant C57BL6/J background. Animals were further backcrossed to the C57BL6/J genetic background for six consecutive generations before using them for experiments. These mice display a mild renal injury compared with other genetic backgrounds (51). Genotyping of COX-2 knockout mice was done as described previously (19). Mice were housed at The Biomedical Laboratory, University of Southern Denmark. All procedures conformed to the Danish national guidelines for the care and handling of animals and the published guidelines from the National Institutes of Health.

WD experiments. Nineteen wild-type and 17 COX-2$^{-/-}$ adult mice (8–10 wk old) were maintained in mouse metabolic cages for the duration of the study, under controlled temperature and light conditions (12:12-h light-dark cycles). The mice had free access to water and food and were acclimatized for 3 days before the experiments. Body weight, food intake, drinking water consumption, urine volume, and baseline urinary osmolality were monitored for 2 consecutive days. For WD experiments, mice were deprived by removing the water bottles for 24 h followed by measurement of urine volume and urinary osmolality; spot urine samples were obtained before and after removal of water bottles. At the end of each experiment, mice were anesthetized and blood was collected by heart puncture. Plasma was separated by centrifugation at 3,000 *g* for 10 min. Plasma osmolality was determined by freeze-point depression (Osmomat 030, Gonotec, Berlin, Germany). Measurement of plasma sodium was done by flame photometry (model IL 943, Instrumentation Laboratory, Lexington, MA). Urea was determined kinetically as the amount of NADH consumed over time measured spectrometrically (UV) after hydrolysis of urea by urase and the formation of L-glutamate by glutamate dehydrogenase (ABX Pentra Urea CP, ABX Diagnostics). Plasma concentration of creatinine was measured by application of dry matter chemistry (Vitros 950, Johnson&Johnson).

Medullary osmolality and sodium concentration. Tissue was processed according to a method developed by Schmidt-Nielsen et al. (45) as modified by Fenton et al. (17). Briefly, kidneys were removed and each individual inner medullas (IM) were rapidly excised, frozen in liquid nitrogen, and stored at −80°C. During the analysis, IM were placed in preweighed tubes. Samples were weighed immediately and subsequently dried over a desiccant at 60°C for 4 h (after which weight remained constant). After reweighing, 100 μl of distilled water was added to each tube, and tubes were capped, boiled in water bath for 5 min, and, after brief centrifugation, stored at 4°C for 24 h for diffusion. After centrifugation for 1 min at 8,000 *g*, supernatant osmolality was determined with the osmometer (Osmomat 030, Gonotec, Berlin, Germany) and sodium was determined by flame photometry (IL 943, flame photometer, Instrumentation Laboratory, Milan, Italy).

Measurements of cAMP and PGE_2. Urine samples were diluted in EIA buffer and assayed directly. cAMP content was measured using a nonradioactive enzyme immunoassay kit (Cayman Chemical, Ann Arbor, MI).

To measure PGE_2 in the brain, tissue samples were homogenized in 0.1 M phosphate buffered saline, pH 7.4, containing 1 mM EDTA and 10 μM indomethacin. Urine samples were diluted in EIA buffer and assayed directly. PGE_2 was measured using a commercial enzyme immunoassay kit (Cayman Chemical).

AVP measurement. Mice were anesthetized, and the cerebrum was removed in total. The region containing the hypothalamus was identified by macroscopic characteristics and a tissue block of ~5 × 5 × 5 mm was removed bilaterally and snap frozen. Tissue was homogenized on ice in sucrose-imidazol buffer (0.3 mol/l sucrose, 25 mmol/l imidazol, 1 mmol/l EDTA, pH adjusted to 7.2 with HCl). Before use, the following was added: pefabloc, leupeptin, Na-ortho-vanadate, NaF, and okadaic acid. After homogenization, the sample was centrifuged at 6,000 rpm for 10 min at 4°C and the supernatant was recovered and stored at −80°C. Protein concentration was measured with a Bradford protein assay. Plasma was obtained from chronically instrumented mice as described in detail below. Blood plasma and the tissue homogenate were extracted and assayed by RIA as described below.

Mouse plasma AVP RIA. For collection of blood samples, chronic indwelling catheters were placed in the femoral artery as described previously (27, 35). The catheters consisted of a Micro-renathane tip (0.38-mm OD) connected to polyethylene tubing. Following the operation, the catheters were attached to a swivel enabling the mice to move freely. To maintain catheter patency, a heparin solution (100 IU/ml in isotonic glucose) was infused at 10 μl/h. The mice recovered for 4 days before the blood samples were taken. These were obtained in heparin-coated tubes and kept on ice. Plasma was separated by centrifugation at 4°C and stored at −80°C until analysis. In all assays, the same human plasma pool was used to determine recovery (mean 72%) and intra-assay variation (6%, $n = 7$). Interassay variation was 5%. The RIA had a detection limit of 0.16 pg/tube (≈0.15 fmol/tube). In other mammals, the physiologically relevant plasma levels include subpicomolar concentrations (3). A 25-g mouse contains ~2 ml of blood. A priori, it was assumed that no more than 10% of blood volume should be withdrawn from a mouse to avoid a blood pressure-related release of AVP. From a 200-μl blood sample, ~80 μl plasma can be obtained. Based on this, it was assumed that plasma should be pooled from at least three mice to provide one sample of the size necessary to allow valid estimations of resting AVP concentrations in the subpicomolar range. Blood samples were taken within 20 s from the arterial catheter of conscious, undisturbed mice. We obtained 3 WT mouse plasma samples for determination of resting AVP concentration by pooling ~150-μl blood samples from a total of 12 mice. One plasma sample from resting COX-2$^{-/-}$ mice was obtained by pooling plasma from $n = 3$ resting COX-2$^{-/-}$ mice. The plasma samples were extracted and assayed as described. Next, experiments were designed to test whether consecutive sampling in the freely moving mouse alters plasma vasopressin ($n = 3$). Four samples of 150–180 μl blood each were obtained in rapid succession from a single mouse. Plasma was extracted and assayed as described. For measurement of AVP after WD, a total of 26 mice (14 WT and 12 COX-2$^{-/-}$) were implanted with catheters as described. After 4 days, mice were water deprived for 24 h and a single blood sample of ~150 μl was rapidly taken. Plasma was extracted and was pooled from two mice. This procedure yielded $n = 7$ and $n = 6$ independent measurements of plasma AVP in WT and COX-2$^{-/-}$ mice, respectively, after WD.

Assay procedures were conducted essentially as described previously (5, 15). In brief, mouse plasma was extracted using Sep-Pak C_{18} cartridges (Waters). Samples were acidified and applied to the conditioned Sep-Pak cartridges. After washing of the cartridges, the samples were eluted using 60% ethanol in 4% acetic acid. The samples were collected in tubes containing Triton X-100 and evaporated to dryness under a stream of air in a 25°C water bath overnight. The content of AVP in the extracts was measured by conventional RIA using an antibody (AB3096) produced in this laboratory. Samples were counted in a gamma counter (Cobra TM,

Table 1. *Primer sequences for qPCR*

COX-2 sense	ggcgttcaactgagctgt	238 bp
COX-2 antisense	ggaattctcactggcttatgtagag	
AVP sense	cgctctccgcttgtttcct	65 bp
AVP antisense	tgggcagttctggaagtagca	
18S sense	ctgtggtaattctagagc	157 bp
18S antisense	aggttatctagagtcacc	

COX, cyclooxygenase.

Table 2. *Baseline measurements in male and female wild-type and COX-2$^{-/-}$ mice*

	Male WT	Male COX-2$^{-/-}$	Female WT	Female COX-2$^{-/-}$
Average body weight, g/day	25.1 ± 0.4	23.1 ± 0.9	21.2 ± 0.2	19.8 ± 1.7
Food intake, g·20 g body wt^{-1}·day^{-1}	3.4 ± 0.03	3.8 ± 0.10	3.8 ± 0.2	4.0 ± 0.2
Feces, g·20 g body wt^{-1}·day^{-1}	1.9 ± 0.03	2.1 ± 0.06	2.2 ± 0.17	2.09 ± 0.2
Na^+ excretion, μmol·day^{-1}·20 g body wt^{-1}	90.6 ± 4.7	201.2 ± 33.6*	74.9 ± 13.2	86.3 ± 5.5
K^+ excretion, μmol·day^{-1}·20 g body wt^{-1}	613 ± 16.1	710 ± 91.4	522 ± 35.2	555 ± 49

Values are means ± SE for n = 6–10 animals/group. WT, wild-type. *$P < 0.05$ vs. COX-2$^{-/-}$.

Auto Gamma, Packard). The results are not corrected for incomplete recovery.

Isolation of RNA and PCR. Total RNA was isolated from the hypothalamic region using an RNeasy minikit (Qiagen). cDNA synthesis, PCR analysis, and qPCR experiments were done as previously described (39). For qPCR experiments, a standard curve was constructed by plotting threshold cycle (Ct values) against serial dilutions of purified PCR product. Specificity of the product was confirmed by postrun melting-point analysis and by gel electrophoresis. Primer sequences are listed in Table 1.

Semiquantitative immunoblotting and immunohistochemistry. The cortex and IM were homogenized and the homogenate was centrifuged at 1,000 *g* for 15 min at 4°C, and the supernatant was used for immunoblotting (38). Samples were run on 9 and 12% polyacrylamide gels (Bio-Rad Protean II), electroeluted to nitrocellulose membranes, and subjected to immunolabeling (38). For immunohistochemistry, the kidneys were perfusion-fixed through the abdominal aorta and samples were prepared, embedded in paraffin, and processed for immunohistochemistry as has been described in detail (38) by using previously characterized antibodies. Photos were captured with a Lecia DMRE camera (Leica Microsystem, Herlev, Denmark) and processed using Photoshop CS5. For morphometry, kidney sections labeled for AQP2 were photographed and compound pictures of whole sections were assembled using Photoshop CS5.

Primary antibodies. For semiquantitative immunoblotting and immunohistochemistry, we used specific antibodies to renal COX-1 and COX-2 (Cayman Chemical, Ann Arbor, MI). Antibodies to AQPs, UT-A1, V2R, and NKCC2, which had been well characterized in previous studies, were as follows: AQP2 (H7661) (37), pSer256-AQP2 (KO407) (9), AQP-3 (LL178AP) (13), V2R (7251AP) (16), NKCC2 (LL320AP) (14), and UT-A1 (17).

Statistical analysis. Statistical comparisons between WT and COX-2$^{-/-}$ mice were analyzed by an unpaired Student's *t*-test when two groups were compared and by one-way ANOVA followed by a post hoc unpaired Student's *t*-test with Bonferroni correction when several

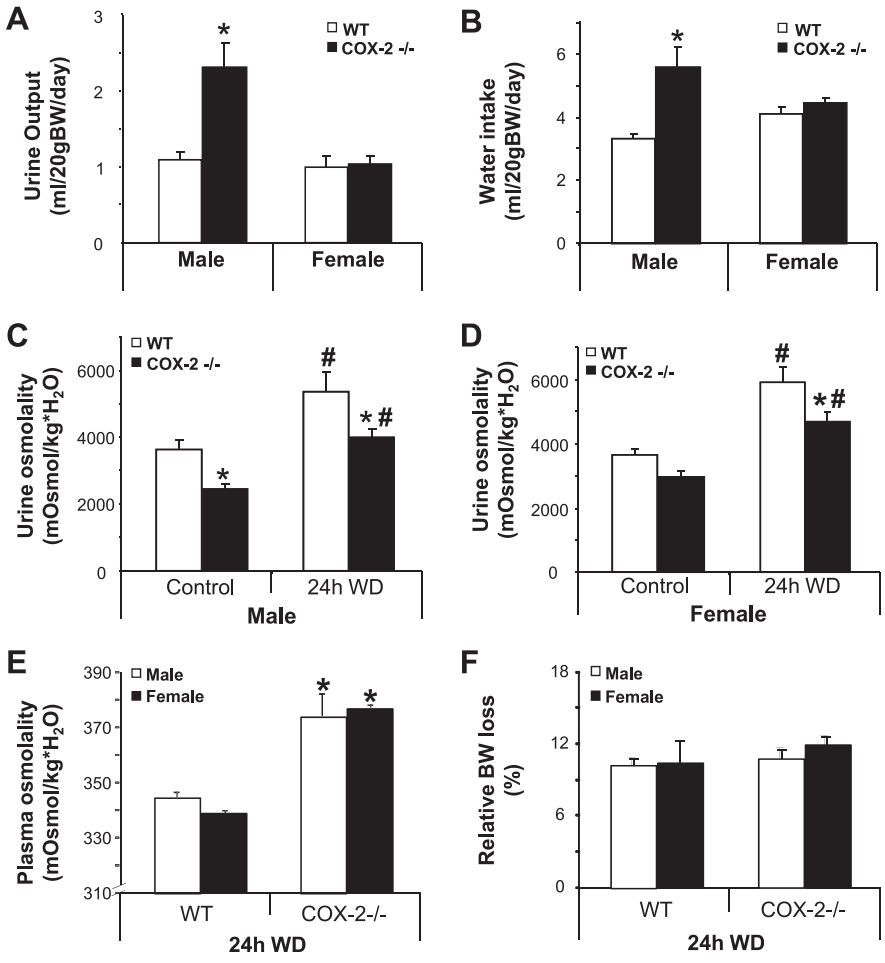

Fig. 1. Urine concentrating ability of wild-type (WT) and cyclooxygenase-2 knockout (COX-2$^{-/-}$) mice. Male and female mice were housed in metabolic cages for 3 days before measurements. Baseline urine output (ml·20 g body wt^{-1}·day^{-1}; *A*) and water intake (ml·20 g body wt^{-1}·day^{-1}; *B*) were measured daily. Values are means ± SE derived from 2 consecutive days using 19 WT and 17 COX-2$^{-/-}$ adult mice (8–10 wk old). *$P < 0.05$ comparing WT with COX-2$^{-/-}$. Water deprivation (WD) was initiated by removal of water bottles from cages of WT and COX-2$^{-/-}$ mice. Spot urine samples were obtained at 0- and 24-h time points. Urine osmolality was measured in both spot urine samples and in urine samples from the urine collection tubes. Data from male (*C*) and female (*D*) were analyzed separately. Plasma osmolality (*E*) and loss of body weight (*F*) were measured in both male and female mice after 24-h WD (24h WD). Values are means ± SE of 36 mice in total. *$P < 0.05$ comparing WT with COX-2$^{-/-}$. #$P < 0.05$ comparing control with 24h WD.

groups were compared. $P < 0.05$ was taken as significant. Data are expressed as means ± SE.

RESULTS

Food and water metabolism in COX-2$^{-/-}$ mice. There was no difference in physical appearance, body weight at entry, food intake, feces excretion, or behavior between adult C57BL/6 COX-2$^{-/-}$ mice and WT littermate controls or between genders (Table 2). At baseline, urinary sodium excretion was significantly higher in male COX-2$^{-/-}$ mice compared with all other groups (Table 2). Daily urine output and water consumption were significantly higher in male COX-2$^{-/-}$ mice than in WT male mice (Fig. 1, *A* and *B*). Female COX-2$^{-/-}$ mice did not differ from WT in baseline urine output and water consumption (Fig. 1, *A* and *B*).

Impaired urine concentrating ability in COX-2$^{-/-}$ mice. Baseline urine osmolality was significantly lower in male COX-2$^{-/-}$ mice than in WT (Fig. 1*C*) whereas there was no difference between the genotypes in female mice (Fig. 1*D*). Following WD, urine osmolality increased significantly in both male and female WT mice as well as in COX-2$^{-/-}$ mice. Male and female COX-2$^{-/-}$ mice achieved the same maximal urine osmolality which was significantly lower than the value reached in WT littermate male and female mice (Fig. 1*C* and 1*D*). Plasma osmolality was significantly higher in both male and female COX-2$^{-/-}$ mice compared with WT mice after WD, and there was no difference between genders (Fig. 1*E*). Relative body weight loss in response to WD did not differ between male and female mice (Fig. 1*F*).

Effect of WD on AVP mRNA and peptide in hypothalamus and plasma of WT and COX-2$^{-/-}$ mice. In response to WD, COX-2 mRNA abundance did not change in hypothalamic tissue (Fig. 2*A*) but the PGE_2 tissue concentration was higher in COX-2$^{-/-}$ than in WT littermates after WD (Fig. 2*B*). Under baseline conditions, there was no difference between genotypes in the AVP mRNA levels in the hypothalamus (Fig. 2*C*). In response to WD, AVP mRNA level increased significantly in COX-2$^{-/-}$ and WT mice compared with baseline (Fig. 2*C*). In the control situation, hypothalamic AVP peptide content was significantly higher in COX-2$^{-/-}$ mice of both genders compared with WT mice (Fig. 2*D*). After WD, total AVP content did not change; i.e., the AVP peptide level in the COX-2$^{-/-}$ mice remained significantly higher than in WT (Fig. 2*D*, genders have been pooled for clarity).

Serial plasma samples obtained from single normohydrated, freely moving WT mice showed that the two first determina-

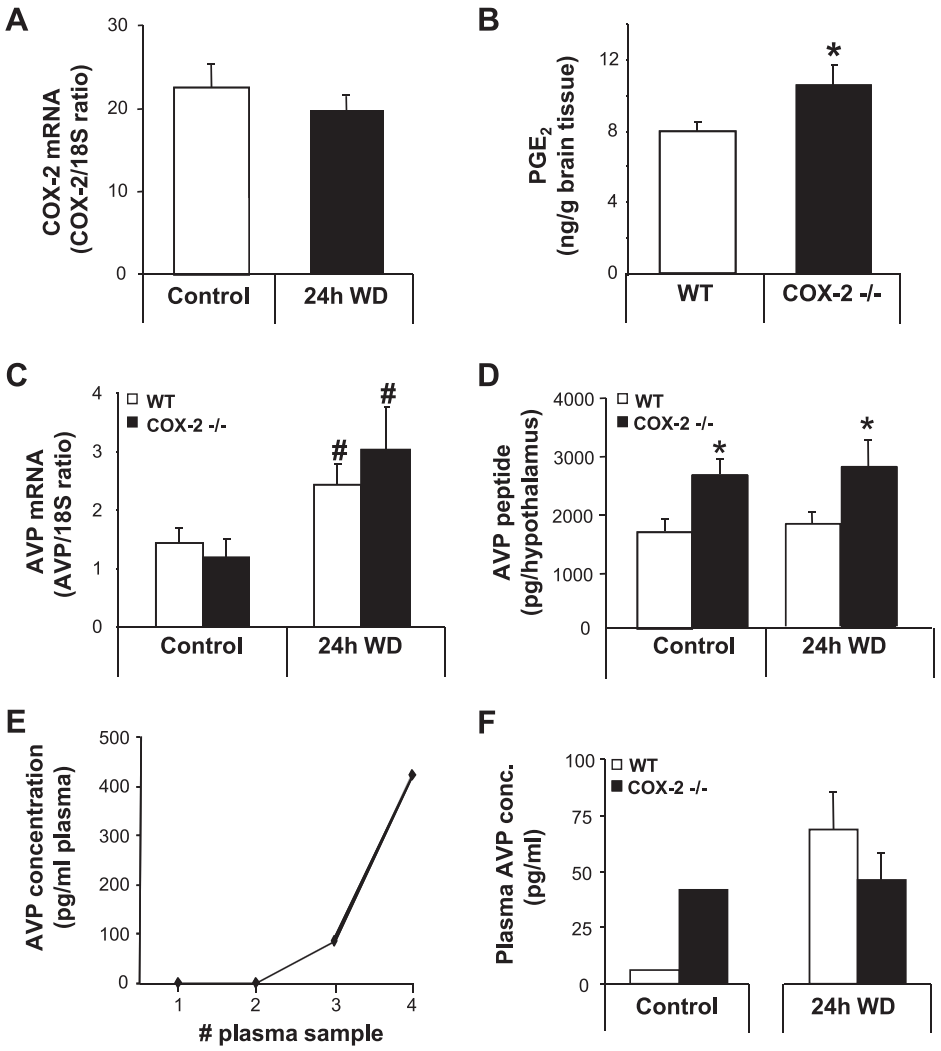

Fig. 2. Effect of WD on AVP concentration in hypothalamus and plasma of WT and COX-2$^{-/-}$ mice. Hypothalamic regions were excised, and total RNA was extracted. *A*: WT mice were subjected to WD for 24 h, and COX-2 mRNA level was measured by qPCR. Values are means ± SE of $n = 6$ mice/group. *B*: PGE_2 content in brains from WD WT and COX-2$^{-/-}$ mice. Values are means ± SE of 11 WT and 7 COX-2$^{-/-}$ mice. *$P < 0.05$ comparing WT with COX-2$^{-/-}$. Hypothalamic AVP mRNA (*C*) and peptide concentration (*D*) in WT and COX-2$^{-/-}$ WD mice. Values are means ± SE of 6 mice/group. *$P < 0.05$ comparing WT with COX-2$^{-/-}$. #$P < 0.05$ comparing control with 24h WD. *E*: AVP content was measured in 4 blood samples (150–180 μl), which were obtained in rapid succession. *F*: plasma AVP content in normohydrated and WD WT and COX-2$^{-/-}$ mice. Plasma AVP content was assayed by radioimmunoassay. Values are means ± SE of normohydrated: WT $n = 12$ (pooled from 4 separate mice 3 times) and COX-2$^{-/-}$ $n = 3$ (pooled from 3 separate mice 1 time) as well as WD: WT $n = 14$ and COX-2$^{-/-}$ $n = 12$ (pool from 2 separate mice 7 and 6 times, respectively) mice/group.

tions were below the detection limit (values <2–3 pg/ml). AVP levels rose to 85 and 421 pg/ml in the third and fourth sample, respectively (Fig. 2*E*). This pattern was observed in three mice. Therefore, single plasma samples were pooled from four separate mice. This was done 3 times, for a total of 12 mice. Resting plasma AVP concentration was 4.4 ± 2 pg/ml (Fig. 2*F*). Baseline plasma AVP concentration was increased in COX-$2^{-/-}$ mice compared with WT (Fig. 2*F*). After 24-h WD, plasma AVP did not differ between the two genotypes (Fig. 2*F*). Of note, plasma AVP concentration in COX-$2^{-/-}$ mice did not change between baseline and WD although this could not be statistically evaluated.

Effect of WD on renal IM interstitial osmolality, NKCC2, UT-A1, and COX expressions in COX-$2^{-/-}$ and WT mice. COX-$2^{-/-}$ and WT mice were used to measure IM interstitial osmolality as well as Na^+ and urea concentration. Normohydrated COX-$2^{-/-}$ mice had a higher interstitial fluid osmolality in the IM compared with WT (Fig. 3*A*). In response to WD, renal IM interstitial osmolality increased significantly in both COX-$2^{-/-}$ and WT mice with no difference between the genotypes (Fig. 3*A*). There was no difference between genotypes in IM interstitial Na^+ concentration at baseline, and it increased to similar levels in WT and COX-$2^{-/-}$ mice in response to WD (Fig. 3*B*). Renal IM interstitial urea concentration in COX-$2^{-/-}$ was higher at baseline and increased in both COX-$2^{-/-}$ and WT after WD (Fig. 3*B*). Furthermore, the urea transporter UT-A1 protein level was increased in IM of COX-$2^{-/-}$ mice compared with WT mice at baseline. In response to WD, UT-A1 protein level was increased in WT, but unchanged in COX-$2^{-/-}$ mice (Fig. 3*C*). In normohydrated COX-$2^{-/-}$ mice, NKCC2 protein in cortex-outer medulla tissue was reduced to 50% of that in WT mice (Fig. 3*D*). WD increased NKCC2 protein abundance by a factor of 2 in WT mice but by a factor of 5 in COX-$2^{-/-}$ to reach a level identical to that of WT mice (Fig. 3*D*). In WT mice, COX-2 protein abundance increased by WD in IM tissue (Fig. 4*A*). In the COX-$2^{-/-}$ mice, COX-2 protein was not detectable in IM (Fig. 4*B*). COX-1 protein abundance was increased in IM tissue in COX-$2^{-/-}$ compared with WT (Fig. 4*C*). Baseline urinary PGE_2 excretion was similar in WT and COX-$2^{-/-}$ and increased significantly by WD in WT. This increase was absent in COX-$2^{-/-}$ mice (Fig. 4*D*).

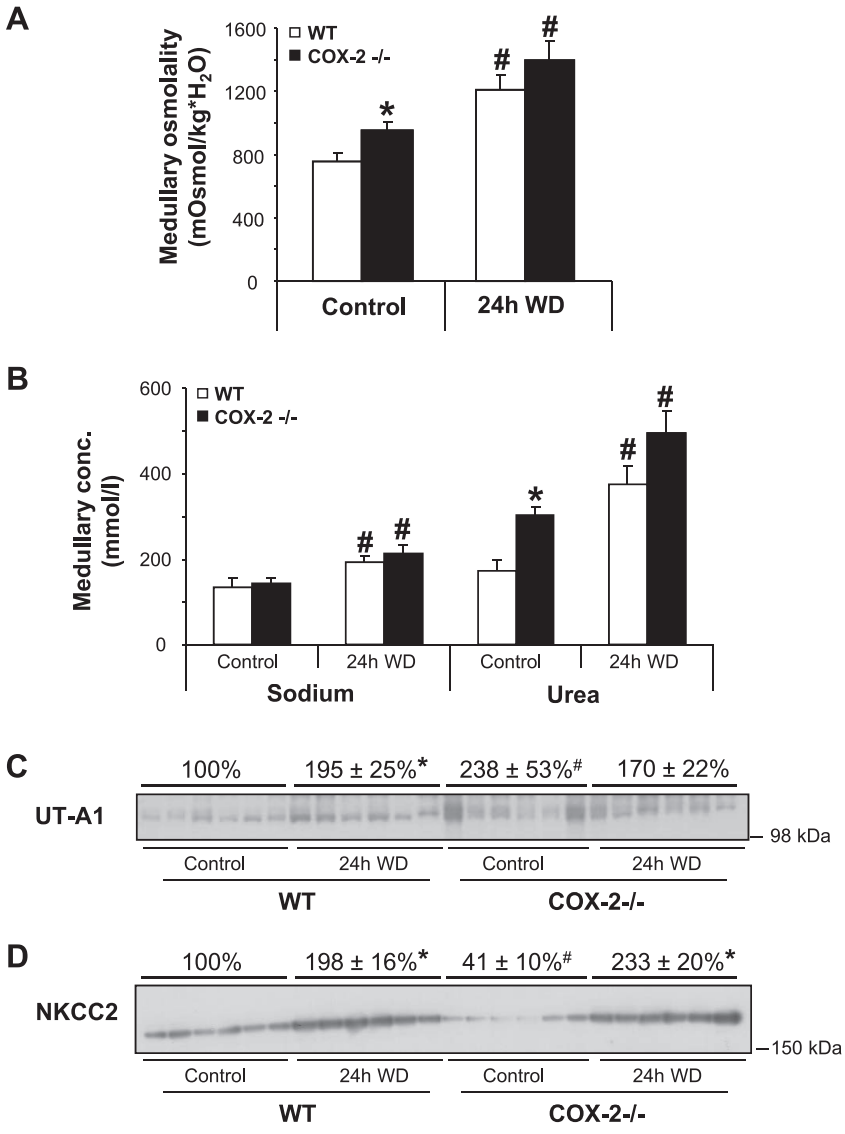

Fig. 3. Effect of WD on renal inner medullary interstitial osmolality, sodium and urea concentration, and expression of urea transporter UT-A1 and Na-K-2Cl cotransporter (NKCC2). Renal inner medullary interstitial tissue osmolality (*A*) and sodium and urea concentration in interstitial fluid (*B*) in WD WT and COX-$2^{-/-}$ mice are shown. *C*: immunoblot analysis for UT-A1 protein abundance in inner medulla of control and WD WT and COX-$2^{-/-}$ mice. *D*: NKCC2 expression in cortex and outer medulla tissue in WD WT and COX-$2^{-/-}$ mice. Values are means ± SE of $n = 6$ mice/group. *$P < 0.05$ comparing WT with COX-$2^{-/-}$. #$P < 0.05$ comparing control with 24h WD.

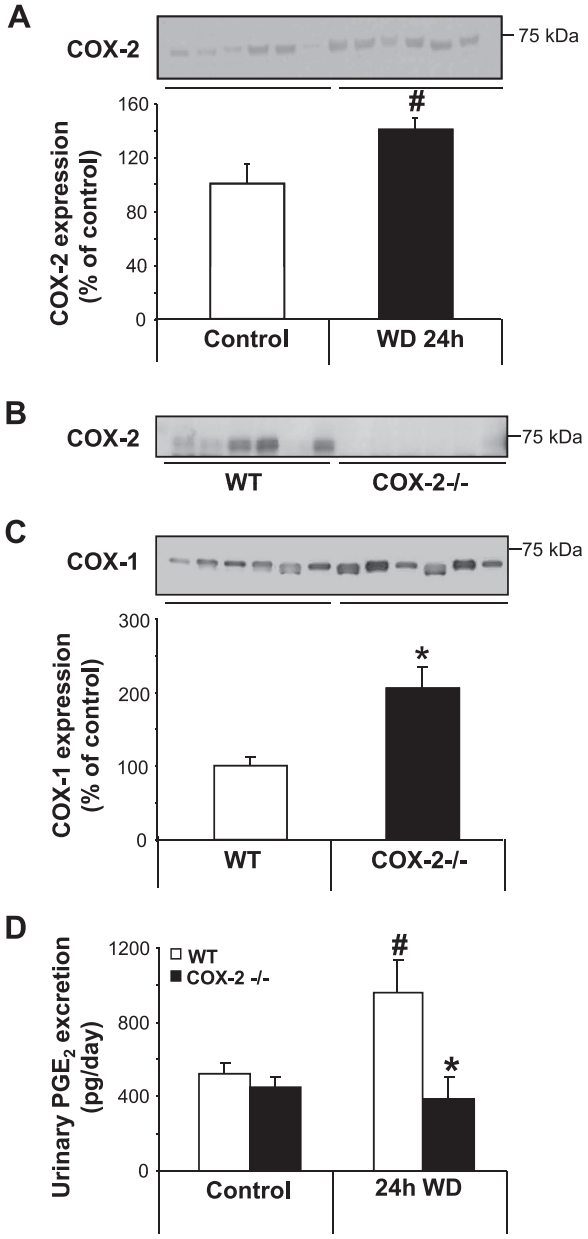

Fig. 4. COX expression and activity in WD WT and COX-2$^{-/-}$ mice. *A*: immunoblot analysis and summary of all the data for COX-2 expression in inner medullary tissue in WD WT mice. *B*: immunoblot analysis for COX-2 expression in inner medullary tissue in WT and COX-2$^{-/-}$ mice. *C*: immunoblot analysis and summary of all the data for COX-1 expression in inner medullary tissue in WT and COX-2$^{-/-}$ mice. *D*: urinary PGE_2 excretion in WD WT and COX-2$^{-/-}$ mice. Values are means ± SE of $n = 6$ mice/group. *$P < 0.05$ comparing WT with COX-2$^{-/-}$. #$P < 0.05$ comparing control with 24h WD.

Effect of WD on cAMP level and renal AVP V2R expression. Urinary excretion of cAMP was not different between genotypes at baseline. After WD, cAMP excretion was significantly lower in COX-2$^{-/-}$ than in WT mice (Fig. 5*A*). V2R protein abundance in IM was significantly decreased in COX-2$^{-/-}$ mice compared with WT mice at baseline and in response to WD (Fig. 5*B*). COX-2 deletion had no effect on EP4 receptor transcript levels in the renal IM (Fig. 5*C*).

Effect of WD on collecting duct AQP abundance and trafficking in WT and COX-2$^{-/-}$ mice. In IM, total AQP2 protein abundance was not different between genotypes and water regimens (Fig. 6*A*). pSer256-AQP2 abundance in IM was not different between COX-2$^{-/-}$ and WT mice at baseline (Fig. 6*B*). WD increased pSer256-AQP2 abundance similarly in WT and COX-2$^{-/-}$ in IM (Fig. 6*B*). Immunolabeling for total AQP2 and pSer256-AQP2 was associated with more intense labeling in the apical membranes of principal cells in the COX-2$^{-/-}$ mice compared with WT at baseline (Fig. 6, *E* and *I* vs. *C* and *G*). WD conferred a noticeable shift of both AQP2 and pS256-AQP2 to the apical membranes in the principal cells from COX-2$^{-/-}$ and WT mice, and no difference in labeling intensity was observed (Fig. 6, *D–F* and *H–J*). There was no difference in AQP3 protein abundance in IM in response to WD in WT mice (Fig. 7*A*). AQP3 protein abundance was higher in IM in COX-2$^{-/-}$ mice at baseline and further increased in response to 24-h WD (Fig. 7*A*). Immunolabeling for AQP3 protein was associated with the basolateral membranes of principal cells, and labeling was more intense in

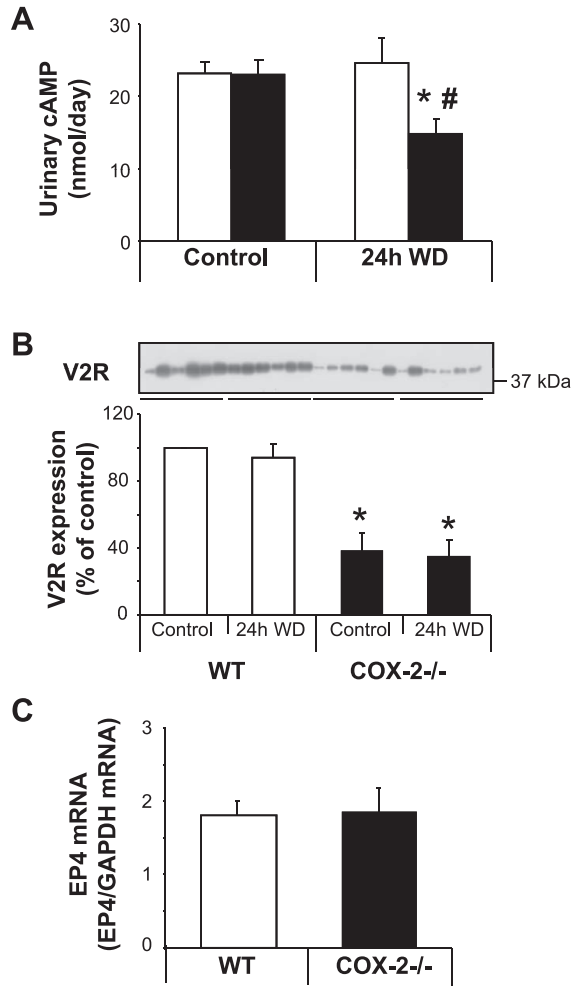

Fig. 5. Effect of water deprivation on urinary cAMP level and renal vasopressin V2 receptor (V2R) expression. *A*: cAMP levels were measured in the urine of WT and COX-2$^{-/-}$ mice WD for 24 h. *B*: immunoblot analysis and summary of all the data for V2R expression in inner medullary tissue in WD WT and COX-2$^{-/-}$ mice. *C*: qPCR of EP4 receptor mRNA levels in WD WT and COX-2$^{-/-}$ mice. Values are means ± SE of $n = 6$ mice/group. *$P < 0.05$ comparing WT with COX-2$^{-/-}$. #$P < 0.05$ comparing control with 24h WD.

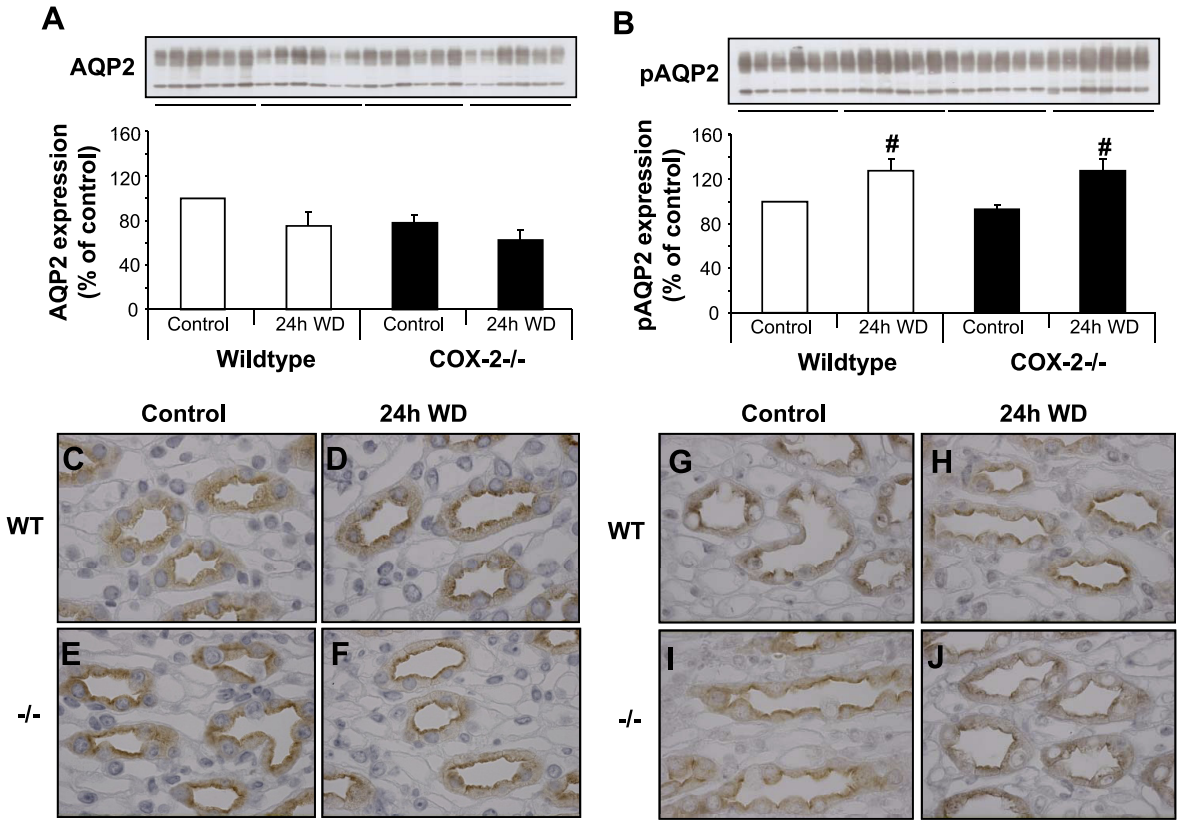

Fig. 6. Renal inner medullary aquaporin-2 (AQP2) and phospho-S256AQP2 water channel abundance and trafficking in WD WT and COX-2$^{-/-}$ mice. Immunoblot analysis and summary of all the data for AQP2 (*A*) and phospho-S256AQP2 (*B*) expression in inner medullary tissue in WD WT and COX-2$^{-/-}$ mice and immunolabeling for inner medullary AQP2 (*C–F*) and phospho-S256AQP2 (*G–J*) in renal sections (×63 magnification) of WD WT and COX-2$^{-/-}$ mice are shown. Values are means ± SE of $n = 6$ mice/group. #$P < 0.05$ comparing control with 24h WD.

COX-2$^{-/-}$ mice (Fig. 7, *D* and *E* vs. *B* and *C*). In the renal cortex-outer medulla fraction, AQP2 and AQP3 protein abundance was increased in normohydrated COX-2$^{-/-}$ kidneys compared with WT. Water deprivation increased total AQP2, phospho-Ser256-AQP2 and AQP3 significantly in both genotypes. Of note, AQP2 and AQP3 levels increased above levels in water-deprived WT mice (Fig. 8).

Renal morphology in COX-2$^{-/-}$ mice. Images of histological sections encompassing all kidney regions including the papilla from COX-2$^{-/-}$ and WT mice are shown in Fig. 9. No tissue injury was apparent in COX-2$^{-/-}$ mice judged by the size of the medulla, the papilla, and by the density of the collecting ducts in the papilla outlined by immunohistochemical labeling for AQP2. A rough, nonstereological, observer-blinded counting of AQP2-positive IM collecting duct profiles supported this observation (COX-2$^{-/-}$: 334 ± 41 vs. WT: 263 ± 12, $n = 3$/group). In the cortex, small glomeruli in the subcapsular region and juxtamedullary glomerular hypertrophy were observed in both male and female COX-2$^{-/-}$ mice compared with WT mice (Fig. 9, *B* and *C*). Plasma creatinine and urea levels were increased in male and female COX-2$^{-/-}$ mice compared with WT mice (14.7 ± 2.4 vs. 7.3 ± 1.1 μmol/l, $P < 0.05$ and 4.9 ± 0.26 vs. 24.6 ± 6.5 mmol/l, $P < 0.05$, respectively).

DISCUSSION

The present data show that homozygous deletion of COX-2 (COX-2$^{-/-}$) in mice attenuates urine concentrating ability and increases hypothalamic AVP peptide content at baseline with a preserved ability to increase hypothalamic AVP mRNA upon WD. Plasma AVP is increased in COX-2$^{-/-}$ mice at baseline along with increased protein abundance of AQP2, AQP3, and UT-A1. In response to WD, WT raised plasma AVP 12-fold while COX-2$^{-/-}$ mice showed no change. There was a male propensity for increased baseline water turnover in COX-2$^{-/-}$ mice, as previously reported (51), but the impairment in urine concentration capacity, developmental glomerular injury, and increased hypothalamic and plasma vasopressin as well as plasma urea and creatinine levels were similar between genders in COX-2$^{-/-}$. Thus the WD challenge uncovers a similar phenotype in male and female COX-2$^{-/-}$ mice that is compensated under baseline conditions in female mice. It has previously been demonstrated that basal water and sodium turnover is unaffected in COX-2$^{-/-}$ on a mixed genetic background (40). In the study by Norwood et al. (40), genders were not analyzed separately, which might explain the discrepancy between the data sets. Similar to the present observation, Yang et al. (51) observed a male propensity for kidney injury and hypertension in COX-2$^{-/-}$ mice. Stereological counting of glomeruli could potentially show minor developmental injury in females or functional differences in hormone action.

These results demonstrate that hypothalamic COX-2 activity is not necessary for regulation of vasopressin by physiological variations in fluid balance and that renal COX-2 activity appears to exert a region-specific suppression of AQP2 and AQP3. The mild defect in urine concentrating ability in COX-

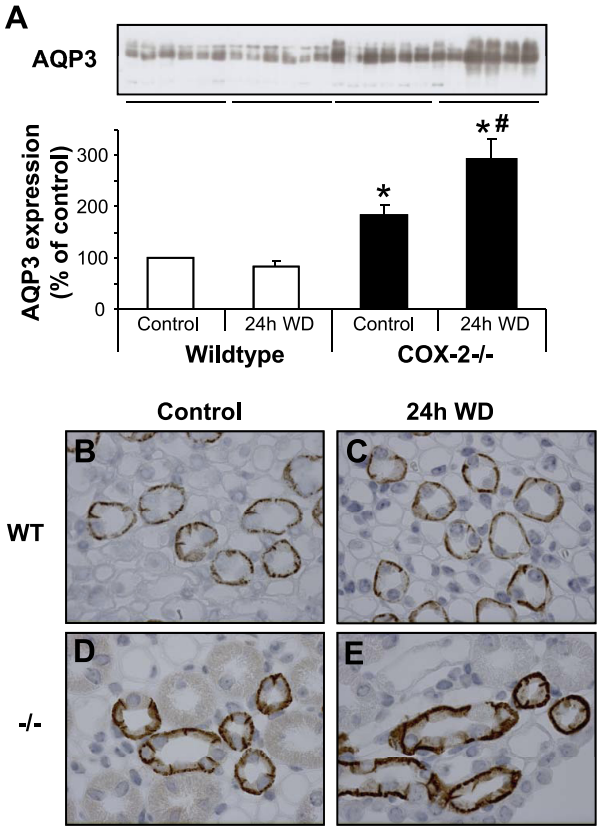

Fig. 7. Renal inner medullary AQP3 water channel abundance and trafficking in WD WT and COX-2$^{-/-}$ mice. Immunoblot analysis and summary of all the data for AQP3 (*A*) expression in inner medullary tissue in WD WT and COX-2$^{-/-}$ mice and immunolabeling for inner medullary AQP3 (*B–E*) in renal sections (×63 magnification) of WD WT and COX-2$^{-/-}$ mice are shown. Values are means ± SE of $n = 6$ mice/group. *$P < 0.05$ comparing WT with COX-2$^{-/-}$. #$P < 0.05$ comparing control with 24h WD.

2$^{-/-}$ mice is likely nephrogenic and could originate from the developmental nephron injury and increased flow in fewer nephrons.

AVP secretion. The data show that rapid removal of 450 μl of blood from C57BL/6 mice is associated with a massive stimulation of AVP secretion. Further blood loss up to a total of 600–700 μl blood (~30% of estimated total blood volume) increases plasma AVP by ~400 times. In humans, plasma AVP may increase by several orders of magnitude following sudden decreases in arterial blood pressure (43, 44). Small blood samples from single conscious mice and subsequent pooling yielded resting AVP plasma concentrations in the ~3–5 pg/ml range. Previous investigations of blood obtained after rapid decapitation of normally hydrated, pentobarbital-anesthetized mice have provided values of 3.3 ± 0.6 pg/ml (36). The present data exemplify that the resting levels of plasma AVP in the mouse are similar to values ~1 pmol/l common to other species and that hypovolemia (most likely via the associated hypotension) may increase the resting levels >100-fold.

Increased central AVP stores and plasma AVP in COX-2$^{-/-}$ mice. Pituitary stores of AVP are rapidly depleted in response to increased plasma osmolality (2). In some, but not all studies (31, 48), PGE_2 directly stimulates AVP secretion in vivo and in vitro (23, 28), and PGE_2-EP1 receptor interaction may account for the effect (30). Since cerebral tissue PGE_2 concentration was elevated in COX-2$^{-/-}$ mice at baseline, COX-2 is not essential for cerebral PGE_2 synthesis. The data are compatible with an intact, and therefore COX-2-independent, central osmosensing mechanism. The increased total content of hypothalamic AVP peptide and increased plasma AVP concentration suggest a tonically increased drive on AVP synthesis and release in COX-2$^{-/-}$ mice at baseline. Data are consistent with an increased effect of AVP on the kidney in COX-2$^{-/-}$ mice at baseline: higher medullary interstitial osmolality, increased accumulation of urea and higher protein abundance of UT-A1 in IM, increased protein abundance of AQP2 (cortex/outer

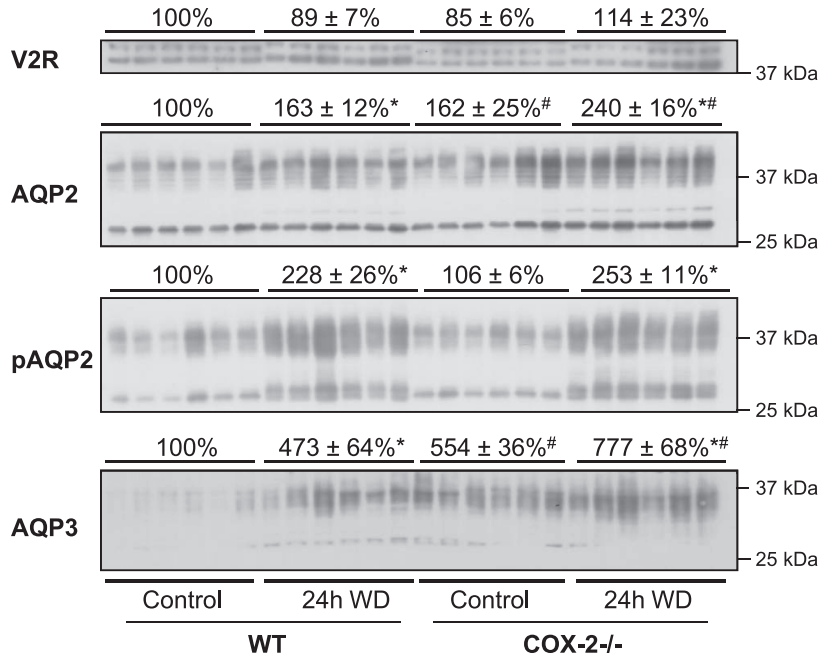

Fig. 8. Cortical and outer medullary fraction of V2R, AQP2, phospho-Ser256-AQP2, and AQP3 water channel abundance in WD WT and COX-2$^{-/-}$ mice. Immunoblot analysis and summary of all the data for V2R, AQP2, phospho-Ser256-AQP2, and AQP3 expression in cortex and outer medullary tissue in WD WT and COX-2$^{-/-}$ mice are shown. Values are means ± SE of $n = 6$ mice/group. *$P < 0.05$ comparing WT with COX-2$^{-/-}$. #$P < 0.05$ comparing control with 24h WD.

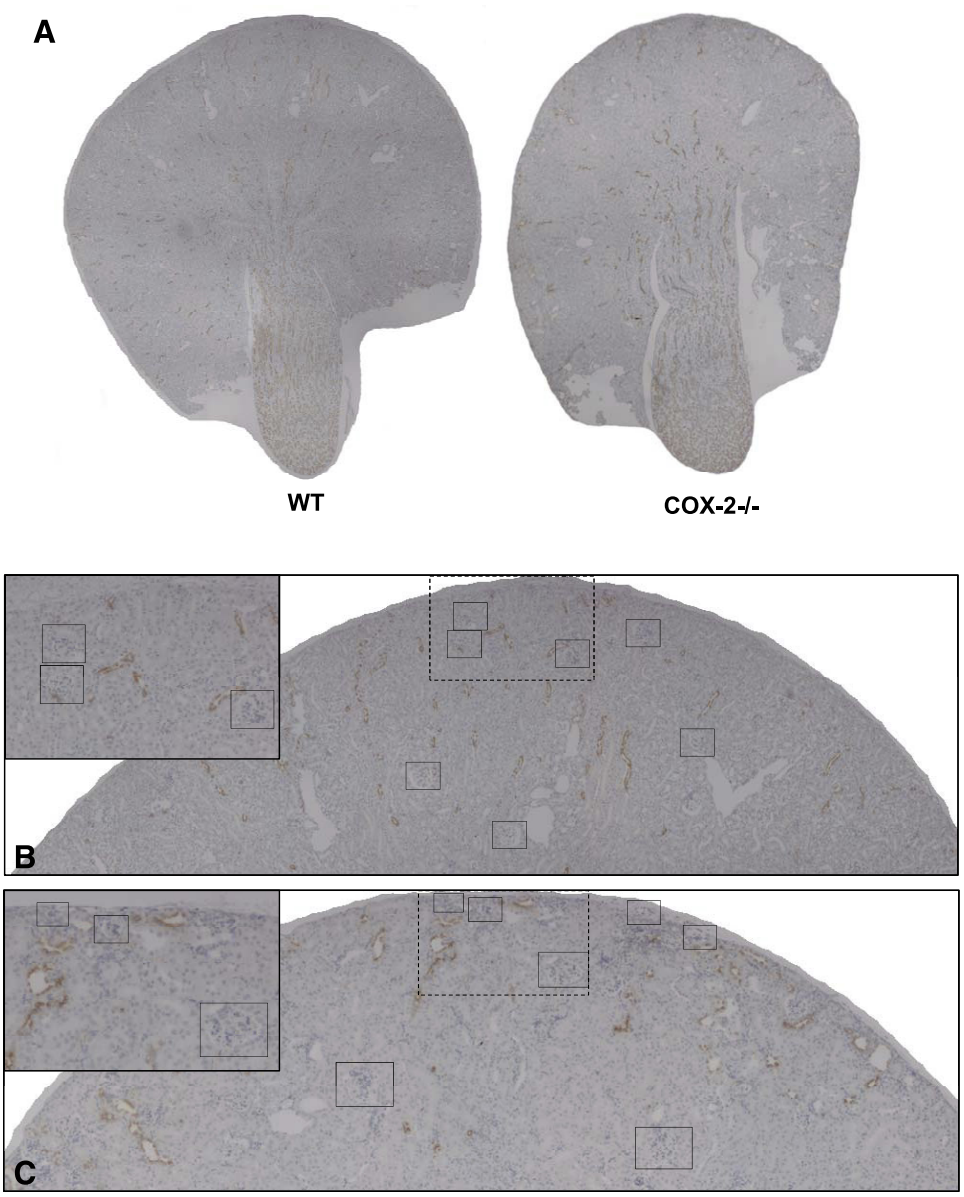

Fig. 9. Renal morphology in WT and COX-$2^{-/-}$ mice. *A*: compound micrographs show coronal sections of kidneys from WT (*left*) and COX-$2^{-/-}$ (*right*) mice labeled for AQP2. *B*: cortical kidney section of male WT mice. *C*: cortical kidney section of male COX-$2^{-/-}$ mice. The rectangular boxes enclose glomeruli in the subcapsular and juxtamedullary cortical region.

medulla fraction) and AQP3 (cortex/outer medulla and IM), and downregulation of the V2R (26). V2R display ligand-mediated internalization (26), and AQP3 is regulated primarily by long-term AVP stimulation (13). The similarity between the plasma AVP concentrations in COX-$2^{-/-}$ and WT mice after WD in the face of a more severe dehydration in COX-$2^{-/-}$ indicates a degree of AVP release impairment or a release process running at maximal capacity. Release of AVP after osmostimulation is under the inhibitory control of glucocorticoids and GABA (6, 47) which might be altered in COX-$2^{-/-}$ mice: in addition, peripheral degradation by peptidases could also be augmented (7, 20). The diminished urinary cAMP excretion in COX-$2^{-/-}$ mice despite similar AVP levels implied attenuated Gs-receptor-coupled responses in the renal medulla, whether caused by reduced abundance of the V2R or by lower PGE_2 synthesis.

COX-2 dependent regulation of AQP2 and -3. After WD, protein abundance of total AQP2 in the cortex/outer medulla and AQP3 in all regions was increased in COX-$2^{-/-}$ compared with WT mice despite similar plasma AVP levels. This difference is therefore likely to be caused by local effects in the renal medulla. Consistent with previous data, baseline PGE_2 excretion was unchanged in COX-$2^{-/-}$ mice (41). This could be explained by little impact of COX-2 activity on PGE_2 in mouse renal medulla at baseline, or by increased expression of COX-1 and increased substrate supply channeled through this pathway in the absence of COX-2. After WD, the urinary PGE_2 excretion was increased in WT mice, but not in COX-$2^{-/-}$ mice. Urinary PGE_2 excretion is mainly derived from medullary synthesis (34). It is concluded that the enhanced renal medullary PGE_2 synthesis after WD is mediated solely by COX-2. The observations are compatible with relief from suppression by COX-2/PGE_2 of AQP2 and AQP3 in water-deprived states in vivo. The increased medullary interstitial osmolality could, along with elevated vasopressin, drive the upregulation of AQP2 in the outer medulla from COX-$2^{-/-}$ mice at baseline (32).

Significance of medullary interstitial fluid osmotic gradient and morphological changes. Global disruption of COX-2 in mice leads to a developmental shortage of last-generation nephrons in the outermost cortex (40). This was observed also with the present, C57BL/6 background where the kidney cortex of the COX-2$^{-/-}$ mice showed characteristic changes with accumulation of small glomeruli in the subcapsular region. The first-generation nephrons later become juxtamedullary nephrons and are intact in COX-2$^{-/-}$ mice (52). This agrees well with the morphologically intact papilla with no difference in the density of collecting ducts and full capacity to generate a hypertonic interstitium in the COX-2$^{-/-}$ mice. An elevated interstitial osmolality was observed at baseline and was due primarily to accumulation of urea. Baseline plasma AVP was elevated in COX-2$^{-/-}$ mice, and this could provide the explanation. In addition, local COX-2 activity promotes medullary blood flow (42), which counteracts accumulation and trapping of osmolytes within the medullary interstitium.

Role of collecting duct water transport. Theoretically, a lower density of principal cells in the COX-2$^{-/-}$ mice could contribute to reduced capacity for water reabsorption despite upregulation of aquaporins, but the principal cell-selective immunostainings for AQP2, pSer256-AQP2, and AQP3, for example, showed no differences in cell density. Immunolabeling for total AQP2 and pSer256-AQP2 showed an intact ability to target apical principal cell membranes after WD in the IM of COX-2$^{-/-}$ mice. This shows that COX-2 activity is not necessary for apical targeting of AQP2. Previous data have shown that PGE_2 stimulates water flux in isolated colleting ducts when applied in the absence of AVP (24, 25). PGE_2 exerts antidiuretic effects in vivo in V2R-deficient mice via cAMP-coupled EP4 receptors by AQP2 upregulation (33), and we observed that the expression of the EP4 receptor is unchanged among the WT and COX-2$^{-/-}$ mice. COX blockers attenuate urine concentrating ability in rats (4). Thus a PGE_2-mediated effect to stimulate hydraulic conductivity or support paracellular tight junctions of collecting ducts could theoretically contribute to the present observations in COX-2$^{-/-}$ mice since an abundance or targeting of aquaporins is not a likely cause of the lower urine concentration. The collecting ducts are likely to receive a larger flow in the COX-2$^{-/-}$ mice with lower nephron endowment and, in addition, COX-2$^{-/-}$ mice have impaired renin-angiotensin system activity (50). Together, this could explain the lower urine concentrating ability despite normal or augmented aquaporin levels in COX-2$^{-/-}$ mice.

In summary, the present data show that COX-2-deficient mice have increased hypothalamic vasopressin stores, intact osmosensitivity of central vasopressin expression, elevated baseline plasma AVP, an intact medullary interstitial osmotic gradient, and unchanged or even elevated protein level of renal AVP-regulated salt and water transport proteins. It is concluded that COX-2$^{-/-}$ mice exhibit a mild nephrogenic diabetes insipidus, which we speculate is caused by hyperfiltration in fewer nephrons and/or by lower renin-angiotensin system activity.

ACKNOWLEDGMENTS

The authors thank Gitte Skou, Gitte Kall, Bodil Kristensen, Lis Teush, Inger Merete Paulsen, and Line V. Nielsen for expert technical assistance. The Water and Salt Research Centre at the University of Aarhus is established and supported by the Danish National Research Foundation (Danmarks Grundforskningsfond).

GRANTS

These studies were supported by The Commission of the European Union (EU Action Programs), The Danish Research Council for Health and Disease, The Danish Heart Association, The Lundbeck Foundation, Helen and Ejnar Bjørnow Foundation, The NOVO Nordisk Foundation, and The AP Moller Foundation.

DISCLOSURES

No conflicts of interest, financial or otherwise, are declared by the authors.

REFERENCES

1. **Anderson RJ, Berl T, McDonald KD, Schrier RW.** Evidence for an in vivo antagonism between vasopressin and prostaglandin in the mammalian kidney. *J Clin Invest* 56: 420–426, 1975.
2. **Arima H, Kondo K, Kakiya S, Nagasaki H, Yokoi H, Yambe Y, Murase T, Iwasaki Y, Oiso Y.** Rapid and sensitive vasopressin heteronuclear RNA responses to changes in plasma osmolality. *J Neuroendocrinol* 11: 337–341, 1999.
3. **Baerwolff M, Bie P.** Effects of subpicomolar changes in vasopressin on urinary concentration. *Am J Physiol Regul Integr Comp Physiol* 255: R940–R945, 1988.
4. **Baggaley E, Nielsen S, Marples D.** Dehydration-induced increase in aquaporin-2 protein abundance is blocked by nonsteroidal anti-inflammatory drugs. *Am J Physiol Renal Physiol* 298: F1051–F1058, 2010.
5. **Bie P, Sandgaard NC.** Determinants of the natriuresis after acute, slow sodium loading in conscious dogs. *Am J Physiol Regul Integr Comp Physiol* 278: R1–R10, 2000.
6. **Biewenga WJ, Rijnberk A, Mol JA.** Osmoregulation of systemic vasopressin release during long-term glucocorticoid excess: a study in dogs with hyperadrenocorticism. *Acta Endocrinol (Copenh)* 124: 583–588, 1991.
7. **Burbach JP, Schoots O, Hernando F.** Biochemistry of vasopressin fragments. *Prog Brain Res* 119: 127–136, 1998.
8. **Chou SY, Porush JG, Faubert PF.** Renal medullary circulation: hormonal control. *Kidney Int* 37: 1–13, 1990.
9. **Christensen BM, Zelenina M, Aperia A, Nielsen S.** Localization and regulation of PKA-phosphorylated AQP2 in response to V_2-receptor agonist/antagonist treatment. *Am J Physiol Renal Physiol* 278: F29–F42, 2000.
10. **Cover PO, Slater D, Buckingham JC.** Expression of cyclooxygenase enzymes in rat hypothalamo-pituitary-adrenal axis: effects of endotoxin and glucocorticoids. *Endocrine* 16: 123–131, 2001.
11. **Dinchuk JE, Car BD, Focht RJ, Johnston JJ, Jaffee BD, Covington MB, Contel NR, Eng VM, Collins RJ, Czerniak PM.** Renal abnormalities and an altered inflammatory response in mice lacking cyclooxygenase II. *Nature* 378: 406–409, 1995.
12. **Downey P, Sapirstein A, O'Leary E, Sun TX, Brown D, Bonventre JV.** Renal concentrating defect in mice lacking group IV cytosolic phospholipase A_2. *Am J Physiol Renal Physiol* 280: F607–F618, 2001.
13. **Ecelbarger CA, Terris J, Frindt G, Echevarria M, Marples D, Nielsen S, Knepper MA.** Aquaporin-3 water channel localization and regulation in rat kidney. *Am J Physiol Renal Fluid Electrolyte Physiol* 269: F663–F672, 1995.
14. **Ecelbarger CA, Terris J, Hoyer JR, Nielsen S, Wade JB, Knepper MA.** Localization and regulation of the rat renal Na^+-K^+-2Cl- cotransporter, BSC-1. *Am J Physiol Renal Fluid Electrolyte Physiol* 271: F619–F628, 1996.
15. **Emmeluth C, Drummer C, Gerzer R, Bie P.** Natriuresis in conscious dogs caused by increased carotid [Na^+] during angiotensin II and aldosterone blockade. *Acta Physiol Scand* 151: 403–411, 1994.
16. **Fenton RA, Brond L, Nielsen S, Praetorius J.** Cellular and subcellular distribution of the type-2 vasopressin receptor in the kidney. *Am J Physiol Renal Physiol* 293: F748–F760, 2007.
17. **Fenton RA, Chou CL, Stewart GS, Smith CP, Knepper MA.** Urinary concentrating defect in mice with selective deletion of phloretin-sensitive urea transporters in the renal collecting duct. *Proc Natl Acad Sci USA* 101: 7469–7474, 2004.
18. **Fleming EF, Athirakul K, Oliverio MI, Key M, Goulet J, Koller BH, Coffman TM.** Urinary concentrating function in mice lacking EP3 receptors for prostaglandin E_2. *Am J Physiol Renal Physiol* 275: F955–F961, 1998.
19. **Friis UG, Madsen K, Svenningsen P, Hansen PB, Gulaveerasingam A, Jorgensen F, Aalkjaer C, Skott O, Jensen BL.** Hypotonicity-induced

Renin exocytosis from juxtaglomerular cells requires aquaporin-1 and cyclooxygenase-2. *J Am Soc Nephrol* 20: 2154–2161, 2009.
20. **Gazis D, Sawyer WH.** Elimination of infused arginine-vasopressin and its long-acting deaminated analogue in rats. *J Endocrinol* 78: 179–186, 1978.
21. **Guan Y, Zhang Y, Breyer RM, Fowler B, Davis L, Hebert RL, Breyer MD.** Prostaglandin E_2 inhibits renal collecting duct Na^+ absorption by activating the EP1 receptor. *J Clin Invest* 102: 194–201, 1998.
22. **Hao CM, Komhoff M, Guan Y, Redha R, Breyer MD.** Selective targeting of cyclooxygenase-2 reveals its role in renal medullary interstitial cell survival. *Am J Physiol Renal Physiol* 277: F352–F359, 1999.
23. **Hashimoto H, Noto T, Nakajima T.** Effects of prostaglandin E2 and D2 on the release of vasopressin and oxytocin. *Prostaglandins Leukot Essent Fatty Acids* 36: 9–14, 1989.
24. **Hebert RL, Jacobson HR, Breyer MD.** PGE_2 inhibits AVP-induced water flow in cortical collecting ducts by protein kinase C activation. *Am J Physiol Renal Fluid Electrolyte Physiol* 259: F318–F325, 1990.
25. **Hebert RL, Jacobson HR, Fredin D, Breyer MD.** Evidence that separate PGE_2 receptors modulate water and sodium transport in rabbit cortical collecting duct. *Am J Physiol Renal Fluid Electrolyte Physiol* 265: F643–F650, 1993.
26. **Hocher B, Merker HJ, Durr JA, Schiller S, Gross P, Hensen J.** Internalization of V2-vasopressin receptors in LLC-PK_1 cells: evidence for receptor-mediated endocytosis. *Biochem Biophys Res Commun* 186: 1376–1383, 1992.
27. **Hristovska AM, Rasmussen LE, Hansen PB, Nielsen SS, Nusing RM, Narumiya S, Vanhoutte P, Skott O, Jensen BL.** Prostaglandin E_2 induces vascular relaxation by E-prostanoid 4 receptor-mediated activation of endothelial nitric oxide synthase. *Hypertension* 50: 525–530, 2007.
28. **Ishikawa S, Saito T, Yoshida S.** The effect of prostaglandins on the release of arginine vasopressin from the guinea pig hypothalamo-neurohypophyseal complex in organ culture. *Endocrinology* 108: 193–198, 1981.
29. **Jensen BL, Mann B, Skott O, Kurtz A.** Differential regulation of renal prostaglandin receptor mRNAs by dietary salt intake in the rat. *Kidney Int* 56: 528–537, 1999.
30. **Kennedy CR, Xiong H, Rahal S, Vanderluit J, Slack RS, Zhang Y, Guan Y, Breyer MD, Hebert RL.** Urine concentrating defect in prostaglandin EP1-deficient mice. *Am J Physiol Renal Physiol* 292: F868–F875, 2007.
31. **Knigge U, Kjaer A, Kristoffersen U, Madsen K, Toftegaard C, Jorgensen H, Warberg J.** Histamine and prostaglandin interaction in regulation of oxytocin and vasopressin secretion. *J Neuroendocrinol* 15: 940–945, 2003.
32. **Li C, Wang W, Summer SN, Cadnapaphornchai MA, Falk S, Umenishi F, Schrier RW.** Hyperosmolality in vivo upregulates aquaporin 2 water channel and Na-K-2Cl co-transporter in Brattleboro rats. *J Am Soc Nephrol* 17: 1657–1664, 2006.
33. **Li JH, Chou CL, Li B, Gavrilova O, Eisner C, Schnermann J, Anderson SA, Deng CX, Knepper MA, Wess J.** A selective EP4 PGE2 receptor agonist alleviates disease in a new mouse model of X-linked nephrogenic diabetes insipidus. *J Clin Invest* 119: 3115–3126, 2009.
34. **Lote CJ, Haylor J.** Eicosanoids in renal function. *Prostaglandins Leukot Essent Fatty Acids* 36: 203–217, 1989.
35. **Mattson DL.** Long-term measurement of arterial blood pressure in conscious mice. *Am J Physiol Regul Integr Comp Physiol* 274: R564–R570, 1998.
36. **Morris M, Li P, Callahan MF, Oliverio MI, Coffman TM, Bosch SM, Diz DI.** Neuroendocrine effects of dehydration in mice lacking the angiotensin AT1a receptor. *Hypertension* 33: 482–486, 1999.
37. **Nielsen J, Kwon TH, Praetorius J, Frøkiær J, Knepper MA, Nielsen S.** Aldosterone increases urine production and decreases apical AQP2 expression in rats with diabetes insipidus. *Am J Physiol Renal Physiol* 290: F438–F449, 2006.
38. **Norregaard R, Jensen BL, Li C, Wang W, Knepper MA, Nielsen S, Frøkiær J.** COX-2 inhibition prevents downregulation of key renal water and sodium transport proteins in response to bilateral ureteral obstruction. *Am J Physiol Renal Physiol* 289: F322–F333, 2005.
39. **Norregaard R, Jensen BL, Topcu SO, Nielsen SS, Walter S, Djurhuus JC, Frøkiær J.** Cyclooxygenase type 2 is increased in obstructed rat and human ureter and contributes to pelvic pressure increase after obstruction. *Kidney Int* 70: 872–881, 2006.
40. **Norwood VF, Morham SG, Smithies O.** Postnatal development and progression of renal dysplasia in cyclooxygenase-2 null mice. *Kidney Int* 58: 2291–2300, 2000.
41. **Qi Z, Cai H, Morrow JD, Breyer MD.** Differentiation of cyclooxygenase 1- and 2-derived prostanoids in mouse kidney and aorta. *Hypertension* 48: 323–328, 2006.
42. **Qi Z, Hao CM, Langenbach RI, Breyer RM, Redha R, Morrow JD, Breyer MD.** Opposite effects of cyclooxygenase-1 and -2 activity on the pressor response to angiotensin II. *J Clin Invest* 110: 61–69, 2002.
43. **Sander-Jensen K, Mehlsen J, Secher NH, Bach FW, Bie P, Giese J, Schwartz TW, Trap-Jensen J, Warberg J.** Progressive central hypovolaemia in man–resulting in a vasovagal syncope? Haemodynamic and endocrine variables during venous tourniquets of the thighs. *Clin Physiol* 7: 231–242, 1987.
44. **Sander-Jensen K, Secher NH, Astrup A, Christensen NJ, Giese J, Schwartz TW, Warberg J, Bie P.** Hypotension induced by passive head-up tilt: endocrine and circulatory mechanisms. *Am J Physiol Regul Integr Comp Physiol* 251: R742–R748, 1986.
45. **Schmidt-Nielsen B, Graves B, Roth J.** Water removal and solute additions determining increases in renal medullary osmolality. *Am J Physiol Renal Fluid Electrolyte Physiol* 244: F472–F482, 1983.
46. **Shibuya I, Setiadji SV, Ibrahim N, Harayama N, Maruyama T, Ueta Y, Yamashita H.** Involvement of postsynaptic EP4 and presynaptic EP3 receptors in actions of prostaglandin E2 in rat supraoptic neurones. *J Neuroendocrinol* 14: 64–72, 2002.
47. **Sladek CD, Armstrong WE.** Gamma-aminobutyric acid antagonists stimulate vasopressin release from organ-cultured hypothalamo-neurohypophyseal explants. *Endocrinology* 120: 1576–1580, 1987.
48. **Summy-Long JY, Bui V, Gestl S, Kadekaro M.** Nitric oxide, interleukin and prostaglandin interactions affecting the magnocellular system. *Brain Res* 940: 10–20, 2002.
49. **Yamaguchi K, Hama H, Watanabe K.** Possible roles of prostaglandins in the anteroventral third ventricular region in the hyperosmolality-evoked vasopressin secretion of conscious rats. *Exp Brain Res* 113: 265–272, 1997.
50. **Yang T, Endo Y, Huang YG, Smart A, Briggs JP, Schnermann J.** Renin expression in COX-2-knockout mice on normal or low-salt diets. *Am J Physiol Renal Physiol* 279: F819–F825, 2000.
51. **Yang T, Huang YG, Ye W, Hansen P, Schnermann JB, Briggs JP.** Influence of genetic background and gender on hypertension and renal failure in COX-2-deficient mice. *Am J Physiol Renal Physiol* 288: F1125–F1132, 2005.
52. **Zhang MZ, Wang JL, Cheng HF, Harris RC, McKanna JA.** Cyclooxygenase-2 in rat nephron development. *Am J Physiol Renal Physiol* 273: F994–F1002, 1997.